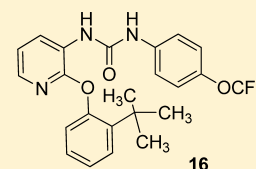


Discovery of 2-(Phenoxypyridine)-3-phenylureas as Small Molecule P2Y₁ Antagonists

Hannguang Chao,* Huji Turdi, Timothy F. Herpin, Jacques Y. Roberge, Yalei Liu, Dora M. Schnur, Michael A. Poss, Robert Rehfuß, Ji Hua, Qimin Wu, Laura A. Price, Lynn M. Abell, William A. Schumacher, Jeffrey S. Bostwick, Thomas E. Steinbacher, Anne B. Stewart, Martin L. Ogletree, Christine S. Huang, Ming Chang, Angela M. Cacace, Meredith J. Arcuri, Deborah Celani, Ruth R. Wexler, and R. Michael Lawrence

Bristol-Myers Squibb Research and Development, P.O. Box 5400, Princeton New Jersey 08543, United States

ABSTRACT: Two distinct G protein-coupled purinergic receptors, P2Y₁ and P2Y₁₂, mediate ADP-driven platelet activation. The clinical effectiveness of P2Y₁₂ blockade is well established. Recent preclinical data suggest that P2Y₁ and P2Y₁₂ inhibition provide equivalent antithrombotic efficacy, while targeting P2Y₁ has the potential for reduced bleeding liability. In this account, the discovery of a 2-(phenoxypyridine)-3-phenylurea chemotype that inhibited ADP-mediated platelet aggregation in human blood samples is described. Optimization of this series led to the identification of compound **16**, 1-(2-(2-*tert*-butylphenoxy)pyridin-3-yl)-3-(4-(trifluoromethoxy)phenyl)urea, which demonstrated a 68 ± 7% thrombus weight reduction in an established rat arterial thrombosis model (10 mg/kg plus 10 mg/kg/h) while only prolonging cuticle and mesenteric bleeding times by 3.3- and 3.1-fold, respectively, in provoked rat bleeding time models. These results suggest that a P2Y₁ antagonist could potentially provide a safe and efficacious antithrombotic profile.



■ INTRODUCTION

The P2Y₁ receptor, a G-protein-coupled receptor, expressed in the heart, skeletal, and various smooth muscles as well as the prostate, brain, and circulating blood cells,¹ is a member of the P2Y family of receptors. The P2Y receptor family is generally considered to consist of eight members, P2Y₁, P2Y₂, P2Y₄, P2Y₆, P2Y₁₁, P2Y₁₂, P2Y₁₃, and P2Y₁₄, encoded by distinct genes, which can be subdivided into two groups based on their coupling to specific G-proteins.² Several studies have suggested that modulators of specific members of the P2Y family could have therapeutic potential for the treatment of a variety of disorders,³ such as diabetes, cancer, and ischemia-reperfusion injury.⁴ Among the P2Y family, P2Y₁ and P2Y₁₂ are of particular interest because they play a major physiological role in ADP-mediated platelet aggregation, an important component of thrombosis.⁵

ADP is a key activator of platelets, and platelet activation is known to play a pivotal role in thrombus formation. ADP activates platelets by simultaneously stimulating P2Y₁ and P2Y₁₂ to produce two separate intracellular signals, which synergize to produce complete platelet activation. The antithrombotic effect of antagonizing the P2Y₁₂ receptor alone is very well validated clinically with the thienopyridines⁶ and other drugs⁷ (Figure 1), but the same level of proof of principle in humans for the P2Y₁ receptor has yet to be demonstrated. In 2001, Léon⁸ first reported that inhibition of P2Y₁ activity alone could lead to an antithrombotic effect in vivo in a model of thromboplastin-induced thromboembolism using both a P2Y₁ knockout mouse and the P2Y₁ antagonist MRS2179.⁹ Subsequently, Jacobson and others described a series of adenine nucleotide-based P2Y₁ receptor antagonists

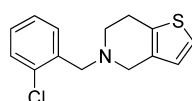
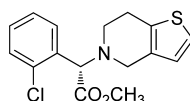
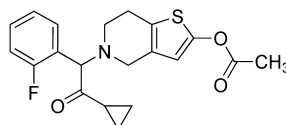
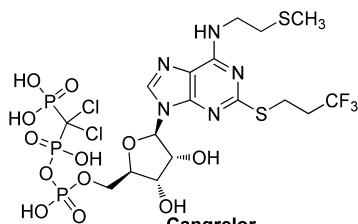
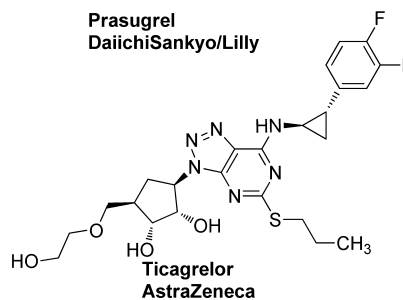
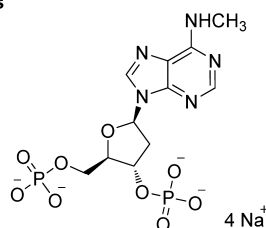
that inhibit ADP-induced platelet aggregation.¹⁰ In general, those adenine nucleotide analogues exhibited good in vitro potency. However, their chemical and enzymatic stabilities are less than desirable, which would be expected to limit their usefulness as oral drug candidates. Thus, the discovery of novel P2Y₁ antagonists with improved pharmaceutical characteristics could have significant utility in the treatment of a variety of thromboembolic disorders.¹¹

■ RESULTS AND DISCUSSION

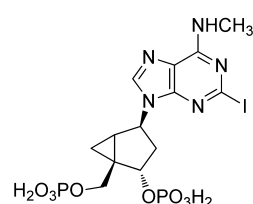
Given the promising evidence that P2Y₁ receptor antagonists may represent a novel antithrombotic strategy that might complement current therapy, a discovery effort to identify small molecule P2Y₁ antagonists was carried out. A high throughput screening effort using the full BMS screening deck (>1 million compounds) against the human P2Y₁ receptor employing a binding assay with [β -³³P]-2-methylthioadenosine diphosphate as the ligand revealed the diaryl urea **1** (Figure 2) with good affinity and binding selectivity toward the P2Y₁ receptor versus P2Y₁₂ (P2Y₁ K_i = 75 nM, P2Y₁₂ K_i > 70 μ M).¹²

The favorable profile of this compound was validated by resynthesis, and it was selected as the starting point for further structural optimization. The modular nature of this compound made it particularly well suited for utilization of array synthesis to efficiently explore the SAR of the chemotype. Optimization efforts began with exploration of the phenyl ring of the urea moiety. Scheme 1 represents the general synthetic route to the targeted compounds. First, reacting 3-CF₃PhOH **2** with 2-

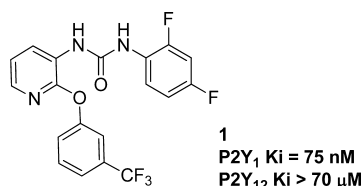
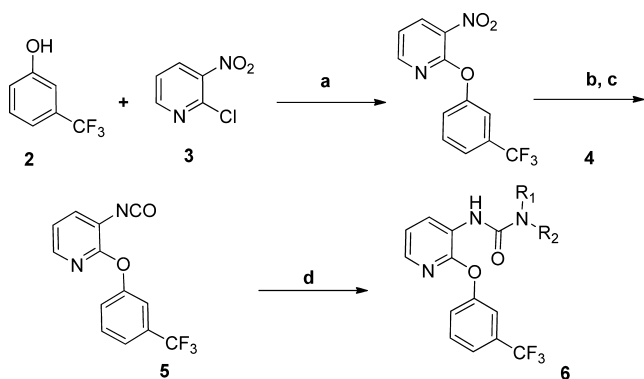
Received: November 27, 2012

P2Y₁₂ antagonistsTiclopidine
SanofiClopidogrel
Sanofi/BMSPrasugrel
DaiichiSankyo/LillyCangrelor
AstraZenecaTicagrelor
AstraZenecaP2Y₁ antagonists

MRS2179



MRS2500

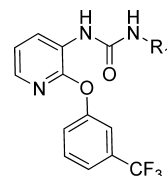
Figure 1. Known P2Y₁₂ and P2Y₁ antagonists.1
P2Y₁ K_i = 75 nM
P2Y₁₂ K_i > 70 μMFigure 2. P2Y₁ lead compound.Scheme 1^a

^aReagents and conditions: (a) Cs₂CO₃, DMF, 80 °C, 14 h, 60%; (b) Zn, NH₄Cl, MeOH, 92%; (c) diphosgene, N¹,N¹,N⁸,N⁸-tetramethylnaphthalene-1,8-diamine, CH₂Cl₂, 100%; (d) 96 R₁R₂NH, THF, 60 °C, yields in range of 12–75%.

chloro-3-nitropyridine 3 in DMF at 80 °C afforded the 3-nitro-2-phenoxy pyridine 4. Subsequent reduction of the nitro group with Zn/NH₄Cl gave the corresponding 3-aminopyridine, which was then reacted with diphosgene in the presence of N¹,N¹,N⁸,N⁸-tetramethylnaphthalene-1,8-diamine to provide the key intermediate isocyanate 5.¹³ In general, the isocyanate derivatives were purified by silica gel chromatography and were

stable up to a year when stored at 0 °C. For subsequent array synthesis, the isocyanate was distributed into 96 vessels and reacted with 96 diverse amines in THF at 60 °C in a parallel format to afford urea analogues 6.

All analogues of type 6 were initially screened in the human P2Y₁ receptor binding assay. This exploration of the distal urea



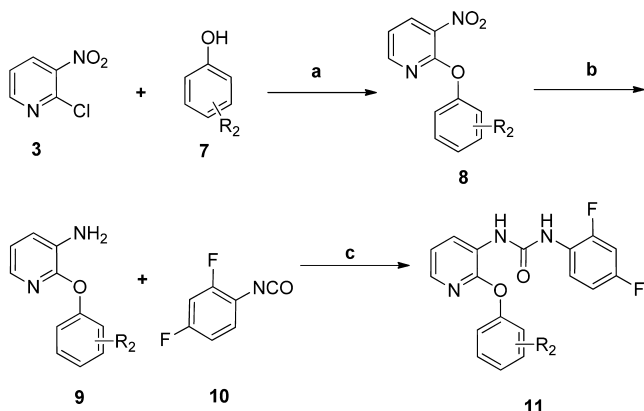
substitution demonstrated that monosubstitution was required for activity. Additionally, aliphatic substituents were not tolerated. Shown in Table 1 are selected examples from the evaluation of the urea phenyl ring. The SAR indicated that substitution of the phenyl ring and the positions of the substitution were critical for P2Y₁ activity. The unsubstituted analogue 6a showed a 3-fold drop in activity compared to the lead 1. Replacement of the *o*-fluorine (6b) with a larger group such as chlorine was not tolerated (6c). Substitution at the meta position was acceptable but, in general, provided less active analogues (6d and 6e). Substitution at the para position with fluorine or chlorine showed comparable activity (6f and 6g), but methyl and methoxy, as well as larger lipophilic groups such as *t*-Bu, OCF₃, or Ph, provided a modest improvement in activity (6h–i). Various other functional groups such as dimethylamine, nitrile, and methyl ester were acceptable at this position but resulted in analogues with weaker binding (6m–o). Bis-substitution was also explored with analogues showing no improvement in activity (6p and 6q). Insertion of one or two methylene groups between the phenyl ring and distal nitrogen atom of the urea resulted in a dramatic loss of activity (6r and 6s).

Table 1. Inhibition Data for Compounds 1 and 6a–s

compd	R ₁	hP2Y ₁ K _i ^a (nM)
1	2, 4-di-F-Ph	75 ± 5
6a	Ph	171 ± 105
6b	2-F-Ph	47 ± 27
6c	2-Cl-Ph	>5000
6d	3-F-Ph	607 ± 105
6e	3-Cl-Ph	128 ± 45
6f	4-F-Ph	145 ± 28
6g	4-Cl-Ph	69 ± 23
6h	4-MePh	48 ± 28
6i	4- <i>t</i> -Bu-Ph	31 ± 4
6j	4-OCF ₃ -Ph	313 ± 198
6k	4-Ph-Ph	28 ± 4
6l	4-OMe-Ph	21 ± 11
6m	4-NMe ₂ -Ph	506 ± 85
6n	4-CN-Ph	571 ± 150
6o	4-CO ₂ Me-Ph	644 ± 296
6p	3,4-di-Cl-Ph	84 ± 16
6q	3,5-di-Cl-Ph	169 ± 38
6r	CH ₂ Ph	>5000
6s	CH ₂ CH ₂ Ph	>5000

^aData represent the mean ± SEM, *n* = 2.

Optimization efforts on the phenoxy ring and the linker were carried out, utilizing the 2,4-difluorophenyl urea present in the HTS hit 1. The same general synthetic scheme was utilized in an array format (Scheme 2), and several analogues were thus

Scheme 2^a^aReagents and conditions: (a) Cs₂CO₃, DMF, 80 °C; (b) Zn, NH₄Cl, EtOH/EtOAc (4:1); (c) toluene, 80 °C, 1.5 h, yields in range of 22–44%.

prepared. Introduction of the variable group in the first step necessitated that all the subsequent steps be carried out in parallel for all vials. Instead of generating an isocyanate of type 5 for each core, 2,4-difluorophenyl isocyanate was condensed with each of 3-aminopyridines.

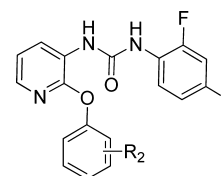
Shown in Table 2 are selected representatives from the exploration of the phenyl ether. As seen with the phenylurea, substituents and their position were pivotal to P2Y₁ activity. The unsubstituted phenyl analogue 11a displayed more than a 30-fold drop in activity compared to compound 1. On the contrary, substitution with a *tert*-butyl group at the ortho position (11b) improved potency by 4-fold, and at the meta position (11c) by 2.5-fold, respectively. Additionally, an

Table 2. Inhibition Data for Compounds 1 and 11a–h

compd	R ₂	hP2Y ₁ K _i ^a (nM)
1	3-CF ₃	75 ± 5
11a	H	2000 ± 1158
11b	2- <i>t</i> -Bu	18 ± 4
11c	3- <i>t</i> -Bu	33 ± 7
11d	2- <i>i</i> -Pr	28 ± 2
11e	2-Et	77 ± 6
11f	2-CF ₃	172 ± 71
11g	4-CF ₃	>5000
11h	4-Me	>5000

^aData represent the mean ± SEM, *n* = 2.

isopropyl group (11d) at the ortho position provided a modest improvement in activity, whereas the ethyl group (11e) displayed the same level of potency as compound 1. Combined, the data indicated that lipophilicity at the ortho position was important for activity. In the case of the CF₃ substituent, while substituting at the ortho position maintained activity (11f) compared to compound 1, moving the CF₃ substituent to the para position (11g) resulted in a substantial loss of activity. This was further confirmed using a methyl group as the para substituent (11h).



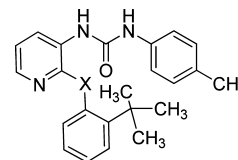
The linker between the phenyl ring and pyridyl ring was explored by replacing the oxygen atom with sulfur or nitrogen. Synthesis of these analogues utilized the same chemistry sequence except that the initial starting phenol was replaced by the correspondingly substituted thiophenol or aniline. When the oxygen atom in compound 12 was replaced by sulfur (13), a modest drop in activity was observed (Table 3). However,

Table 3. Inhibition Data for Compounds 12–15

compd	X	hP2Y ₁ K _i ^a (nM)
12	O	7 ± 0.1
13	S	20 ± 8
14	NH	175 ± 40
15	NMe	>5000

^aData represent the mean ± SEM, *n* = 2.

replacing with nitrogen (14) resulted in a 20-fold drop in activity. Furthermore, methylation of the linking nitrogen of 14 provided a more significant loss in activity (15).



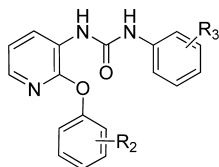
Following the exploration of the two terminal phenyl rings, a focused library was executed based on the discovered SAR, in which preferred substituents at each position were combined. This so-called “best–best” array included eight preferred substituents each from the phenoxy moiety and the phenyl

Table 4. Inhibition, Platelet Aggregation, and Selectivity Data for Compounds 1, 12, and 16–19

compd	R ₂	R ₃	hP2Y ₁ K _i ^a (nM)	hPRP ^b IC ₅₀ (μM)	hP2Y ₁₂ K _i ^a (nM)	hP2Y ₂ K _i ^c (nM)	hP2Y ₆ K _i ^c (nM)	hP2Y ₁₁ K _i ^c (nM)	hP2Y ₁₄ K _i ^a (nM)	metab stab., % remaining (h/r) ^d
1	3-CF ₃	2,4-DiF	75 ± 5	53 ± 28 (n = 5)	>70000	—	—	—	—	75/50
12	2- <i>t</i> -Bu	4-Me	7 ± 0.1	7.2 ± 2.1 (n = 2)	>70000	2700	>15000	>15000	2350 ± 950	33/38
16	2- <i>t</i> -Bu	4-OCF ₃	6 ± 0.6	2.1 ± 0.28 (n = 7)	>70000	>15000	>15000	>15000	3500 ± 1000	80/86
17	2- <i>t</i> -Bu	4- <i>t</i> -Bu	8 ± 0.4	1.2 ± 0.2 (n = 2)	>70000	>15000	>15000	>15000	5950 ± 950	58/33
18	2- <i>i</i> -Pr	4- <i>t</i> -Bu	7 ± 0.3	4.4 ± 3.8 (n = 4)	>70000	>15000	>15000	>15000	>15000	73/35
19	2- <i>i</i> -Pr	4-OCF ₃	16 ± 2	9.4 ± 4 (n = 2)	>70000	6400	>15000	>15000	3300 ± 600	97/80

^aData represent the mean ± SEM, n = 2. ^bPRP run in human platelet-rich plasma using 2.5 μM ADP. ^cn = 1. ^dh: human; r: rat. Compounds (3 μM) were incubated with human or rat liver microsomes (1.0 mg/mL) for 10 min.

ring of the urea moiety. This array was prepared following the same chemistry outlined in Scheme 1. This “best–best” array produced several potent antagonists with a clear trend that preferred the combination of substitution of the phenoxy ring with a lipophilic group, such as *tert*-butyl or isopropyl at the ortho or meta position and substitution of the urea phenyl ring at the para position. Listed in Table 4 are a few selected examples from the array demonstrating that several compounds had single digit nanomolar binding affinity. These compounds were also evaluated in a platelet aggregation assay to assess their ability to block ADP-induced platelet aggregation in human platelet rich plasma¹⁴ with several of these showing single digit micromolar potency. To ensure that this antiplatelet activity was due exclusively to P2Y₁ antagonism, all compounds were tested for their P2Y₁₂ activity. As shown, all compounds had excellent selectivity over P2Y₁₂. Additionally, these compounds also showed good selectivity over other P2Y receptors such as P2Y₂, P2Y₆, P2Y₁₁, and P2Y₁₄ (Table 4).



Compounds with good in vitro P2Y₁ binding affinity and functional activity were evaluated to determine their metabolic stability. Because the in vivo studies were carried out in rats, the metabolic stability in rat became an important factor for compound selection. Among those compounds tested, only compounds 16 and 19 showed reasonable metabolic stability in rats, 86% and 80% remaining after incubation with rat liver microsomes for 10 min, respectively. Although compound 19 was reasonably stable in rats, its functional activity was not quite potent enough for further consideration. The Caco-2 permeability for compound 16 was found to be low (21 nm s⁻¹) as was the aqueous solubility of the hydrochloride salt (<1 μg/mL at pH 6.5). Solubilizing vehicles that were compatible with the in vivo models were used for solution dosing for pharmacokinetic evaluation. The pharmacokinetic profile of compound 16 (Table 5) revealed this compound had reasonable plasma exposure, clearance, and half-life with

moderate oral bioavailability (*F* = 18%) when dosed at 30 mg/kg using 10%EtOH/10% cremophor/80% H₂O as vehicle.

The antithrombotic efficacy of compound 16 was assessed in established arterial thrombosis and bleeding models in male anesthetized rats.¹² As shown in Figure 3, compound 16 clearly improved blood flow and reduced thrombus weight in a dose-dependent manner. A maximum of 68 ± 7% thrombus weight reduction compared to vehicle was observed using a 10 mg/kg bolus followed by 10 mg/kg/h infusion dosing paradigm. Furthermore, vascular occlusion was prevented in all drug-treated rats at this dose. Ex vivo platelet aggregation responses to ADP were also significantly inhibited at all antithrombotic doses. Compound 16 was also tested in provoked bleeding time models. As shown in Figure 4, the highest tested dose of 10 mg/kg plus 10 mg/kg/h prolonged cuticle and mesenteric bleeding times by 3.3- and 3.1-fold over control, respectively. In previous studies using these same rat models, the P2Y₁₂ antagonist clopidogrel, administered as an oral pretreatment dose of 20 mg/kg, reduced arterial thrombus weight by 67 ± 5% and prolonged cuticle and mesenteric bleeding times by 4.1- and 8.2-fold over control, respectively.¹²

CONCLUSIONS

Novel P2Y₁ antagonists have been identified by optimization of a high throughput screening hit. These urea analogues have demonstrated excellent in vitro P2Y₁ antagonist activity. Compound 16 showed inhibition of platelet aggregation in human platelet-rich plasma with no activity toward the P2Y₁₂ receptor. Furthermore, compound 16 provided significant reduction in thrombus weight in a rat arterial thrombosis model with a limited effect on bleeding. The antithrombotic and bleeding profiles of compound 16 were favorable in comparison to the established P2Y₁₂ antagonist clopidogrel,¹⁵ suggesting that the current series of P2Y₁ antagonists may have potential as novel antithrombotic agents.

EXPERIMENTAL SECTION

General Methods. Starting materials, reagents, and solvents were obtained from commercial sources and used as received. All reactions were carried out with continuous stirring under an atmosphere of dry nitrogen. The resonance frequency for ¹H (¹³C) on a Jeol JNM-ECF-500 is 500 MHz (125 MHz) and Bruker Variance 400 is 400 MHz

Table 5. Pharmacokinetic Properties for Compound 16

compd	dosage, mg/kg	C _{max} (nM)	T _{max} (h)	AUC total (nM·h)	CL, mL/min/kg	V _{ss} , L/kg	T _{half} (h)	F (%)
16 ^a	1	160	0.8	169	16	5.6	15.4	7
16 ^b	30	5830	2.0	15900	13	0.8	1.43	18

^aDose: iv: 1 mg/kg (n = 3), po: 1 mg/kg (n = 2), vehicle: 10% DMAC/10% EtOH/10% cremophor/70% H₂O. ^bDose: iv: 1 mg/kg (n = 3), po: 30 mg/kg (n = 2), vehicle: 10% EtOH/10% cremophor/80% H₂O.

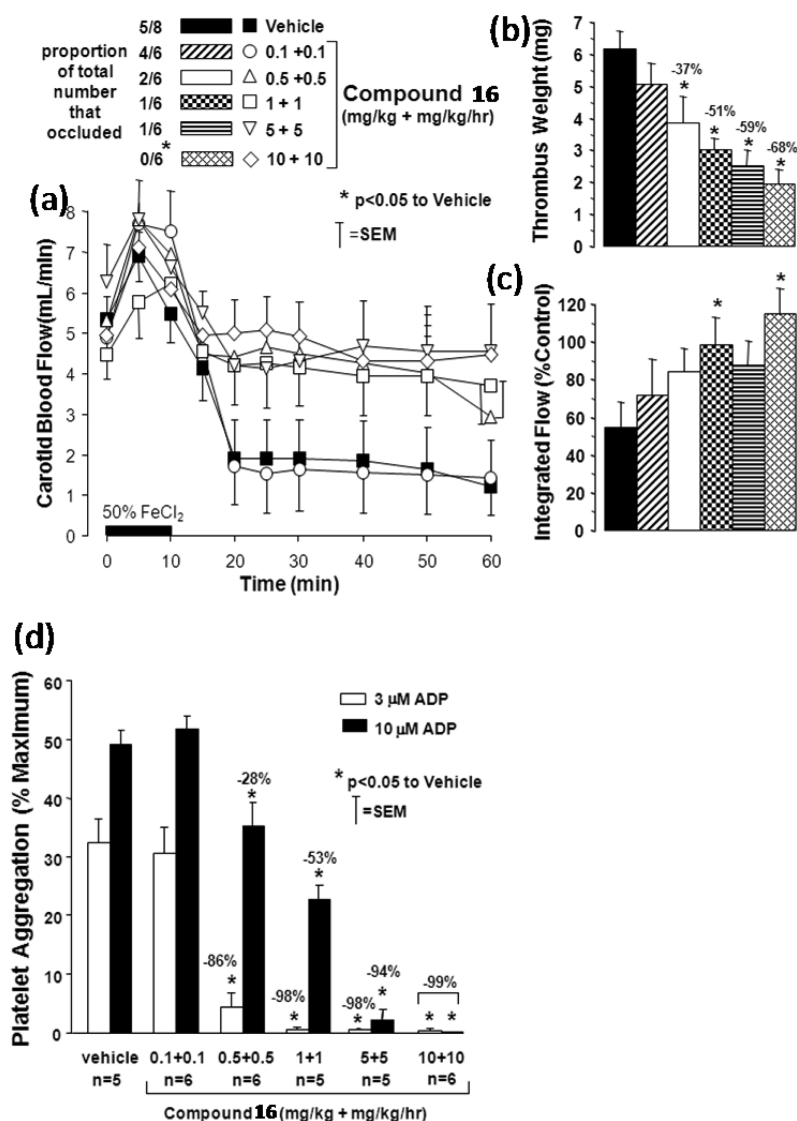


Figure 3. Effect of compound **16** on arterial thrombosis and platelet function in anesthetized rats. Vehicle or compound **16** was dosed as a bolus plus sustaining iv infusion starting 15 min prior to inducing thrombus formation by topical FeCl_2 . (a) Carotid blood flow was measured during thrombus formation. (b) Thrombus weight, (c) integrated blood flow, and (d) ex vivo platelet aggregation responses to ADP were determined at the end of the experiment when platelet counts were sufficient for the assay (resulted in fewer replicates in some groups). Percent reductions in thrombus weight and platelet aggregation are indicated for responses that were significantly different from vehicle. The number of rats in the thrombosis model is indicated in the “proportion of total number that occluded”. Compound **16** doses (mg/kg + mg/kg/h) of 0.1 + 0.1, 0.5 + 0.5, 1 + 1, 5 + 5, and 10 + 10 resulted in plasma concentrations (μM) of 0.4 ± 0.1 , 1.8 ± 0.7 , 4.0 ± 0.2 , 16.5 ± 1.6 , and 36.5 ± 2.5 , respectively.

(100 MHz). Chemical shifts (δ) are reported in ppm downfield from internal tetramethylsilane (TMS), and coupling constants (J) are in hertz (Hz). Peak multiplicities are expressed as follows: singlet (s), doublet (d), doublet of doublets (dd), triplet (t), quartet (q), multiplet (m), broad singlet (br s). TLC was performed on EMD silica gel 60 F_{254} glass plates (2.5×7.5 cm). Microwave reactions were run in a Biotage initiator instrument. Products were analyzed by reverse phase analytical HPLC carried out on a Shimadzu analytical HPLC system running DiscoveryVP software using method A: Phenomenex Luna C18 column (4.6×50 mm) eluted at 4 mL/min with a 4 min gradient from 100% A to 100% B (A: 10% methanol, 89.9% water, 0.1% TFA; B: 10% water, 89.9% methanol, 0.1% TFA, UV 220 nm), method B: Phenomenex Luna C18 column (4.6×50 mm) eluted at 4 mL/min with a 4 min gradient from 100% A to 100% B (A: 10% acetonitrile, 89.9% water, 0.1% TFA; B: 10% water, 89.9% acetonitrile, 0.1% TFA, UV 220 nm), or method C: Zorbax SB C18 column (4.6×75 mm) eluted at 2.5 mL/min with methanol/water with 0.2% H_3PO_4 as a gradient of 10% to 90% methanol over 8 min followed by holding at 90% methanol for 3 min (UV 220 nm). Purification of intermediates

and final products was carried out via either normal or reverse phase chromatography. Normal phase chromatography was carried out on an ISCO CombiFlash System Sqi16x using prepacked SiO_2 cartridges eluted with gradients of hexanes and ethyl acetate. Reverse phase preparative HPLC was carried out using a Shimadzu preparative HPLC system running DiscoveryVP software on a Shim-PackVP-ODS column (50×20 mm) at 20 mL/min, 6 min gradient 100% A to 100% B with the solvent systems used for the analytical procedure. LCMS were obtained on a Shimadzu HPLC system running DiscoveryVP software, coupled with a Waters Model Platform LC mass spectrometer running MassLynx version 3.5 software using the same column and conditions as utilized for analytical procedure described above. Compounds of interest were greater than 95% pure as determined by orthogonal HPLC methods. The analysis was carried out on a Shimadzu HPLC system, equipped with orthogonal columns; Waters sun fire column (C18, $3.5 \mu\text{m}$, 3.0×150 mm) and Waters Xbridge phenyl (C18, $3.5 \mu\text{m}$, 4.6×150 mm) eluted at 2 mL/min with a 12 min gradient from 100% A to 100% B. For low pH, solvent A: 95% H_2O /5% CH_3CN /0.05% TFA; solvent B: 5% H_2O /95%

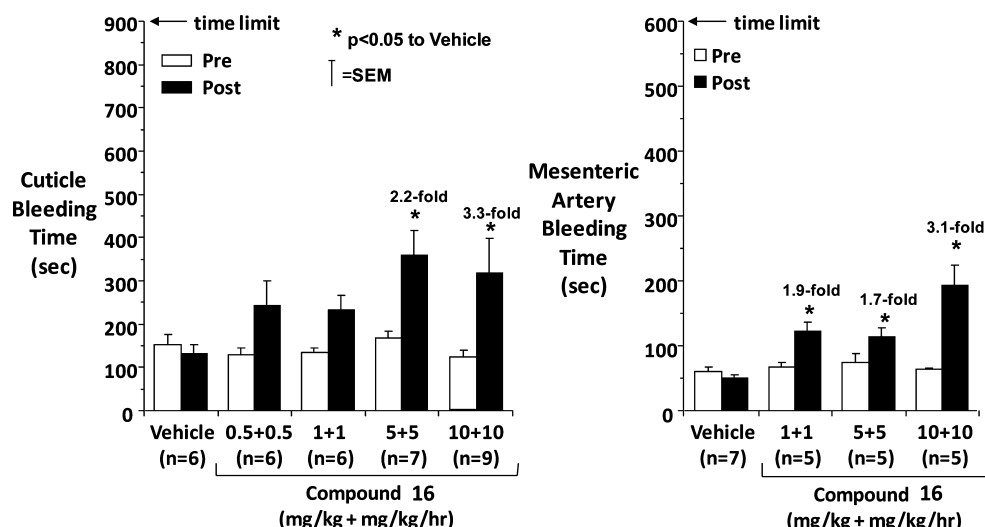


Figure 4. Effect of compound 16 on provoked bleeding times in anesthetized rats. Vehicle or compound 16 was dosed as a bolus plus sustaining iv infusion. Bleeding times were determined before and 15 min after test article administration. Fold increases over control bleeding times are indicated for responses that were significantly different from vehicle.

CH₃CN/0.05% TFA. For high pH, solvent A: 95% H₂O/5% CH₃CN/0.01 M NH₄HCO₃; solvent B: 5% H₂O/95% CH₃CN/0.01M NH₄HCO₃.

1-(2,4-Difluorophenyl)-3-(2-(3-(trifluoromethyl)phenoxy)pyridin-3-yl)urea (1). A solution of 2-chloro-3-nitropyridine 3 (20 g, 125 mmol) in DMF (120 mL) was treated with 3-(trifluoromethyl)-phenol 2 (21 g, 129 mmol) and cesium carbonate (50 g, 154 mmol). The mixture was heated at 70 °C for 14 h. The reaction was cooled to room temperature, and DMF was evaporated. The residue was taken up in EtOAc which was washed with 5% LiCl (3 × 100 mL) and then brine (3 × 100 mL). Drying (MgSO₄) and removal of solvent afforded a brown solid which was recrystallized from ethanol to afford compound 4 as an off-white solid (21 g, 60%). (M + H⁺) = 285.04; ¹H NMR (400 MHz, CD₃OD) δ 7.2 (dd, J = 7.96, 1.39 Hz, 1H), 7.4 (m, 2H), 7.45 (m, 1H), 7.11 (m, 2H), 7.5–7.54 (td, J = 4.93, 1.64 Hz, 1H), 8.48 (dd, J = 7.83, 1.77 Hz, 1H), 8.52 (dd, J = 7.83, 1.77 Hz, 1H).

Compound 4 (21 g, 74 mmol) was dissolved in a 1:4 mixture of methanol and THF (160 mL). Palladium on activated charcoal (10%, 2.1 g, 1.93 mmol) was added, and the mixture was stirred overnight under 1 atm hydrogen pressure. The reaction mixture was filtered over Celite and concentrated to afford a white solid which was recrystallized from EtOAc to afford the 2-(3-(trifluoromethyl)phenoxy)pyridin-3-amine (17.5 g, 92%) as a white powder. (M + H⁺) = 254.3. To a solution of the amine (8.2 g, 34.3 mmol) and diphosgene (5.5 g, 28 mmol) in CH₂Cl₂ (175 mL) at 0 °C was added dropwise a solution of CH₂Cl₂ (125 mL) containing N¹,N¹,N⁸,N⁸-tetramethylnaphthalene-1,8-diamine (14.8 g, 67 mmol). After addition was completed, the resulting mixture was stirred at 0 °C for an additional 45 min and then washed with 0.5 N HCl (3 × 150 mL), 1 N NaOH (2 × 100 mL), and brine. Drying (MgSO₄) and removal of solvent afforded compound 5 as a solid (9.6 g, 100%). This material was used for the subsequent reaction without further purification.

To a solution of isocyanate (5) (28 mg, 1.0 mmol) in toluene (1 mL) in a 2-dram vial was added 2,4-difluoroaniline (16.1 mg, 0.125 mmol). The resulting mixture was heated with shaking at 80 °C for 1.5 h. The solvent was removed by vacuum centrifugation in a speedvac, and the crude product was purified by reverse phase preparative HPLC using CH₃CN/H₂O/TFA solvent system. After removal of solvent in vacuo, the TFA salt of compound 1 was obtained as a white solid (13.0 mg, 32%). ¹H NMR (500 MHz, CD₃OD) δ 6.94 (t, J = 8.80 Hz, 1H), 7.02 (ddd, J = 11.27, 8.52, 2.75 Hz, 1H), 7.13 (dd, J = 7.70, 4.95 Hz, 1H), 7.44 (d, J = 8.25 Hz, 1H), 7.50 (s, 1H), 7.53 (d, J = 7.70 Hz, 1H), 7.62 (t, J = 7.97 Hz, 1H), 7.73 (d, J = 4.95 Hz, 1H), 8.09 (td, J = 9.07, 6.05 Hz, 1H), 8.63 (d, J = 8.25 Hz, 1H). LC-MS (ESI) m/z

410.1 orthogonal HPLC column 1 retention time = 12.12 min, column 2 = 10.29 min.

Compounds 6a–s, 11a–h, 12, and 16–19 were prepared according to the procedures described for 1.

1-Phenyl-3-(2-(3-(trifluoromethyl)phenoxy)pyridin-3-yl)urea (6a). Yield: 23.9 mg (49%). ¹H NMR (400 MHz, CD₃OD) δ 7.03 (t, J = 7.42 Hz, 1H), 7.13 (dd, J = 7.70, 4.95 Hz, 1H), 7.26–7.32 (m, 2H), 7.44 (d, J = 8.25 Hz, 3H), 7.50 (s, 1H), 7.54 (d, J = 7.70 Hz, 1H), 7.63 (t, J = 7.97 Hz, 1H), 7.72 (d, J = 3.30 Hz, 1H), 8.61–8.66 (m, 1H). LC-MS (ESI) m/z 374.0 (M + H⁺); orthogonal HPLC column 1 retention time = 12.04 min, column 2 = 10.56 min.

1-(2-Fluorophenyl)-3-(2-(3-(trifluoromethyl)phenoxy)pyridin-3-yl)urea (6b). Yield: 17.2 mg (44%). ¹H NMR (400 MHz, CD₃OD) δ 7.00–7.06 (m, 1H), 7.09–7.17 (m, 3H), 7.44 (d, J = 8.25 Hz, 1H), 7.48–7.55 (m, 2H), 7.63 (t, J = 7.97 Hz, 1H), 7.73 (d, J = 4.95 Hz, 1H), 8.11–8.18 (m, 1H), 8.65 (d, J = 8.25 Hz, 1H). LC-MS (ESI) m/z 392.0 (M + H⁺); orthogonal HPLC column 1 retention time = 12.40 min, column 2 = 10.79 min.

1-(2-Chlorophenyl)-3-(2-(3-(trifluoromethyl)phenoxy)pyridin-3-yl)urea (6c). Yield: 19.5 mg (48%). ¹H NMR (400 MHz, CD₃OD) δ 7.02–7.08 (m, 1H), 7.14 (dd, J = 7.70, 4.95 Hz, 1H), 7.26–7.31 (m, 1H), 7.40 (d, J = 9.34 Hz, 1H), 7.44 (d, J = 7.70 Hz, 1H), 7.50 (s, 1H), 7.54 (d, J = 8.25 Hz, 1H), 7.63 (t, J = 7.97 Hz, 1H), 7.73 (d, J = 4.95 Hz, 1H), 8.12 (d, J = 8.24 Hz, 1H), 8.63–8.68 (m, 1H). LC-MS (ESI) m/z 408.0 (M + H⁺); orthogonal HPLC column 1 retention time = 12.81 min, column 2 = 11.05 min.

1-(3-Fluorophenyl)-3-(2-(3-(trifluoromethyl)phenoxy)pyridin-3-yl)urea (6d). Yield: 9.8 mg (25%). ¹H NMR (400 MHz, CD₃OD) δ 6.71–6.79 (m, 1H), 7.07 (d, J = 7.70 Hz, 1H), 7.14 (dd, J = 8.24, 4.95 Hz, 1H), 7.23–7.31 (m, 1H), 7.41–7.51 (m, 3H), 7.54 (d, J = 7.70 Hz, 1H), 7.63 (t, J = 7.97 Hz, 1H), 7.72 (d, J = 4.40 Hz, 1H), 8.64 (d, J = 7.70 Hz, 1H). LC-MS (ESI) m/z 392.0 (M + H⁺); orthogonal HPLC column 1 retention time = 12.44 min, column 2 = 10.85 min.

1-(3-Chlorophenyl)-3-(2-(3-(trifluoromethyl)phenoxy)pyridin-3-yl)urea (6e). Yield: 15.5 mg (38%). ¹H NMR (400 MHz, CD₃OD) δ 6.99–7.03 (m, 1H), 7.14 (dd, J = 8.25, 4.95 Hz, 1H), 7.26 (d, J = 5.50 Hz, 2H), 7.44 (d, J = 8.24 Hz, 1H), 7.49–7.56 (m, 2H), 7.62 (d, J = 7.70 Hz, 1H), 7.67 (s, 1H), 7.73 (d, J = 3.30 Hz, 1H), 8.63 (d, J = 6.05 Hz, 1H). LC-MS (ESI) m/z 408.0 (M + H⁺); orthogonal HPLC column 1 retention time = 13.07 min, column 2 = 11.27 min.

1-(4-Fluorophenyl)-3-(2-(3-(trifluoromethyl)phenoxy)pyridin-3-yl)urea (6f). Yield: 14.1 mg (36%). ¹H NMR (400 MHz, CD₃OD) δ 7.04 (t, J = 8.79 Hz, 2H), 7.13 (dd, J = 7.70, 4.95 Hz, 1H), 7.44 (dd, J = 9.07, 4.67 Hz, 3H), 7.50 (s, 1H), 7.54 (d, J = 7.70

Hz, 1 H), 7.63 (t, $J = 7.70$ Hz, 1 H), 7.72 (d, $J = 3.30$ Hz, 1 H), 8.62 (d, $J = 6.60$ Hz, 1 H). LC-MS (ESI) m/z 392.0 ($M + H^+$); orthogonal HPLC column 1 retention time = 10.12 min, column 2 = 9.72 min.

1-(4-Chlorophenyl)-3-(2-(3-(trifluoromethyl)phenoxy)pyridin-3-yl)urea (6g). Yield: 21.6 mg (53%). ^1H NMR (400 MHz, CD_3OD) δ 7.13 (dd, $J = 8.25, 4.95$ Hz, 1 H), 7.25–7.31 (m, 2 H), 7.40–7.48 (m, 3 H), 7.50 (s, 1 H), 7.54 (d, $J = 7.70$ Hz, 1 H), 7.63 (t, $J = 7.97$ Hz, 1 H), 7.72 (d, $J = 4.95$ Hz, 1 H), 8.62 (d, $J = 8.25$ Hz, 1 H). LC-MS (ESI) m/z 408.0 ($M + H^+$); orthogonal HPLC column 1 retention time = 12.95 min, column 2 = 11.19 min.

1-(4-Methylphenyl)-3-(2-(3-(trifluoromethyl)phenoxy)pyridin-3-yl)urea (6h). Yield: 18.06 mg (47%). ^1H NMR (400 MHz, CD_3OD) δ 2.29 (s, 3H), 7.08–7.15 (m, 3H), 7.29–7.34 (m, 2H), 7.40–7.46 (m, 1H), 7.48–7.56 (m, 2H), 7.61 (d, $J = 7.90$ Hz, 1H), 7.71 (dd, $J = 4.80, 1.80$ Hz, 1H), 8.61 (dd, $J = 8.10, 1.80$ Hz, 1H). LC-MS (ESI) m/z 388.1 ($M + H^+$); orthogonal HPLC column 1 retention time = 12.09 min, column 2 = 9.98 min.

1-(4-*tert*-Butylphenyl)-3-(2-(3-(trifluoromethyl)phenoxy)pyridin-3-yl)urea (6i). Yield: 15.9 mg (37%). ^1H NMR (400 MHz, CD_3OD) δ 1.30 (s, 9 H), 7.13 (dd, $J = 7.70, 4.95$ Hz, 1 H), 7.30–7.39 (m, 4 H), 7.44 (d, $J = 8.25$ Hz, 1 H), 7.50 (s, 1 H), 7.54 (d, $J = 7.70$ Hz, 1 H), 7.62 (d, $J = 8.24$ Hz, 1 H), 7.71 (d, $J = 3.30$ Hz, 1 H), 8.62 (d, $J = 6.05$ Hz, 1 H). LC-MS (ESI) m/z 430.1 ($M + H^+$); orthogonal HPLC column 1 retention time = 13.80 min, column 2 = 11.76 min.

1-(4-(Trifluoromethoxy)phenyl)-3-(2-(3-(trifluoromethyl)phenoxy)pyridin-3-yl)urea (6j). Yield: 18.7 mg (41%). ^1H NMR (400 MHz, CD_3OD) δ 7.13 (dd, $J = 7.97, 4.67$ Hz, 1 H), 7.21 (d, $J = 8.25$ Hz, 2 H), 7.44 (d, $J = 8.25$ Hz, 1 H), 7.50 (s, 1 H), 7.52–7.58 (m, 3 H), 7.63 (t, $J = 7.97$ Hz, 1 H), 7.71–7.75 (m, 1 H), 8.63 (d, $J = 9.89$ Hz, 1 H). LC-MS (ESI) m/z 458.0 ($M + H$); orthogonal HPLC column 1 retention time = 13.25 min, column 2 = 11.34 min.

1-(Biphenyl-4-yl)-3-(2-(3-(trifluoromethyl)phenoxy)pyridin-3-yl)urea (6k). Yield: 5.4 mg (12%). ^1H NMR (400 MHz, CD_3OD) δ 7.14 (dd, $J = 8.24, 4.95$ Hz, 1 H), 7.29 (t, $J = 7.42$ Hz, 1 H), 7.38–7.48 (m, 3 H), 7.50–7.67 (m, 9 H), 7.72 (d, $J = 4.95$ Hz, 1 H), 8.65 (d, $J = 8.25$ Hz, 1 H). LC-MS (ESI) m/z 450.0 ($M + H^+$); orthogonal HPLC column 1 retention time = 13.45 min, column 2 = 11.68 min.

1-(4-Methoxyphenyl)-3-(2-(3-(trifluoromethyl)phenoxy)pyridin-3-yl)urea (6l). Yield: 17.3 mg (43%). ^1H NMR (400 MHz, CD_3OD) δ 3.77 (s, 3 H), 6.88 (d, $J = 8.79$ Hz, 2 H), 7.12 (dd, $J = 8.24, 4.95$ Hz, 1 H), 7.33 (d, $J = 9.34$ Hz, 2 H), 7.43 (d, $J = 7.70$ Hz, 1 H), 7.49 (s, 1 H), 7.52–7.56 (m, 1 H), 7.62 (t, $J = 7.97$ Hz, 1 H), 7.71 (d, $J = 4.95$ Hz, 1 H), 8.60 (d, $J = 8.25$ Hz, 1 H). LC-MS (ESI) m/z 404.1 ($M + H^+$); orthogonal HPLC column 1 retention time = 11.68 min, column 2 = 10.32 min.

1-(4-Dimethylaminophenyl)-3-(2-(3-(trifluoromethyl)phenoxy)pyridin-3-yl)urea (6m). Yield: 11.2 mg (27%). ^1H NMR (400 MHz, CD_3OD) δ 3.06 (s, 6 H), 7.13 (dd, $J = 8.25, 4.95$ Hz, 2 H), 7.29–7.37 (m, 1 H), 7.41–7.51 (m, 4 H), 7.52–7.57 (m, 1 H), 7.63 (t, $J = 7.97$ Hz, 1 H), 7.72 (d, $J = 3.30$ Hz, 1 H), 8.61 (d, $J = 6.05$ Hz, 1 H). LC-MS (ESI) m/z 417.0 ($M + H^+$); orthogonal HPLC column 1 retention time = 6.98 min, column 2 = 7.65 min.

1-(4-Cyanophenyl)-3-(2-(3-(trifluoromethyl)phenoxy)pyridin-3-yl)urea (6n). Yield: 14.3 mg (36%). ^1H NMR (400 MHz, CD_3OD) δ 7.14 (dd, $J = 7.70, 4.95$ Hz, 1 H), 7.45 (d, $J = 8.24$ Hz, 1 H), 7.51 (s, 1 H), 7.53–7.57 (m, 1 H), 7.60–7.64 (m, 1 H), 7.66 (s, 4 H), 7.74 (d, $J = 4.95$ Hz, 1 H), 8.62–8.68 (m, 1 H). LC-MS (ESI) m/z 399.0 ($M + H^+$); orthogonal HPLC column 1 retention time = 11.82 min, column 2 = 10.41 min.

Methyl 4-(3-(2-(3-(Trifluoromethyl)phenoxy)pyridin-3-yl)ureido)benzoate (6o). Yield: 22.8 mg (53%). ^1H NMR (400 MHz, CD_3OD) δ 3.87 (s, 3 H), 7.14 (dd, $J = 7.70, 4.95$ Hz, 1 H), 7.45 (d, $J = 8.25$ Hz, 1 H), 7.49–7.66 (m, 5 H), 7.74 (d, $J = 4.95$ Hz, 1 H), 7.96 (d, $J = 8.79$ Hz, 2 H), 8.65 (d, $J = 6.05$ Hz, 1 H). LC-MS (ESI) m/z 432.0 ($M + H^+$); orthogonal HPLC column 1 retention time = 12.09 min, column 2 = 10.48 min.

1-(3,4-Chlorophenyl)-3-(2-(3-(trifluoromethyl)phenoxy)pyridin-3-yl)urea (6p). Yield: 17.26 mg (39%). ^1H NMR (400 MHz, CD_3OD) δ 7.13 (dd, $J = 8.00, 5.00$ Hz, 1H), 7.29 (dd, $J = 8.80, 2.60$ Hz, 1H), 7.38–7.46 (m, 2H), 7.48–7.56 (m, 2H), 7.62 (d, $J = 8.10$ Hz, 1H), 7.73 (dd, $J = 5.00, 1.70$ Hz, 1H), 7.83 (d, $J = 2.40$ Hz, 1H),

8.62 (dd, $J = 8.00, 1.70$ Hz, 1H). LC-MS (ESI) m/z 442.0 ($M + H^+$); orthogonal HPLC column 1 retention time = 14.20 min, column 2 = 11.92 min.

1-(3,5-Chlorophenyl)-3-(2-(3-(trifluoromethyl)phenoxy)pyridin-3-yl)urea (6q). Yield: 33.1 mg (75%). ^1H NMR (400 MHz, CD_3OD) δ 7.06 (s, 1 H), 7.14 (dd, $J = 8.25, 4.95$ Hz, 1 H), 7.44 (d, $J = 8.25$ Hz, 1 H), 7.47–7.52 (m, 3 H), 7.54 (d, $J = 7.70$ Hz, 1 H), 7.63 (t, $J = 7.97$ Hz, 1 H), 7.73 (d, $J = 4.95$ Hz, 1 H), 8.63 (d, $J = 6.05$ Hz, 1 H). LC-MS (ESI) m/z 442.0 ($M + H^+$); orthogonal HPLC column 1 retention time = 14.28 min, column 2 = 11.99 min.

1-Benzyl-3-(2-(3-(trifluoromethyl)phenoxy)pyridin-3-yl)urea (6r). Yield: 10.0 mg (26%). ^1H NMR (400 MHz, CD_3OD) δ 4.41 (s, 2 H), 7.10 (dd, $J = 8.24, 4.95$ Hz, 1 H), 7.21–7.28 (m, 1 H), 7.32 (d, $J = 4.40$ Hz, 4 H), 7.39 (d, $J = 8.25$ Hz, 1 H), 7.45 (s, 1 H), 7.48–7.54 (m, 1 H), 7.60 (t, $J = 7.97$ Hz, 1 H), 7.66–7.71 (m, 1 H), 8.55 (d, $J = 8.25$ Hz, 1 H). LC-MS (ESI) m/z 388.1 ($M + H^+$); orthogonal HPLC column 1 retention time = 11.46 min, column 2 = 10.24 min.

1-Phenethyl-3-(2-(3-(trifluoromethyl)phenoxy)pyridin-3-yl)urea (6s). Yield: 8.1 mg (20%). ^1H NMR (400 MHz, CD_3OD) δ 2.83 (t, $J = 7.15$ Hz, 2 H), 3.46 (t, $J = 7.15$ Hz, 2 H), 7.09 (dd, $J = 7.97, 4.67$ Hz, 1 H), 7.18 (t, $J = 6.87$ Hz, 1 H), 7.22–7.31 (m, 4 H), 7.37 (d, $J = 8.25$ Hz, 1 H), 7.43 (s, 1 H), 7.51 (d, $J = 7.70$ Hz, 1 H), 7.60 (t, $J = 7.97$ Hz, 1 H), 7.67 (d, $J = 4.95$ Hz, 1 H), 8.52 (d, $J = 8.25$ Hz, 1 H). LC-MS (ESI) m/z 402.1 ($M + H^+$); orthogonal HPLC column 1 retention time = 11.79 min, column 2 = 10.46 min.

3-Nitro-2-phenoxy pyridines 8. Forty eight phenols **7** (1.06 mmol each in 1 mL of DMF) were dispensed into 24-well miniblocks. To these solutions was added Cs_2CO_3 (360 mg, 1.1 mmol) to each well followed by 2-chloro-3-nitropyridine (**3**) (158 mg, 1.0 mmol) in DMF (1 mL). The reactions were heated with shaking at 80 °C for 18 h. The reaction mixtures were filtered and collected into 16 × 100 mm test tubes. EtOAc (2 mL) was added to each well, shaken for 2–3 min, and then combined with the DMF filtrate. The combined solutions were dried in speedvac. The crude mixtures were dissolved in EtOAc (2.5–4 mL) and washed with H_2O (2 × 0.6 mL), saturated NaHCO_3 (1 × 0.5 mL), and H_2O (2 × 0.5 mL). Solvents were removed by vacuum centrifugation in a speedvac to afford crude products which were used for the subsequent reaction without further purification.

3-Amino-2-phenoxy pyridines 9. The nitro compounds **8** were dissolved in a 4:1 mixed solution containing absolute EtOH (4 mL) and EtOAc (1 mL). Zn dust (1.3 g, 20 mmol) and NH_4Cl (300 mg, 5.4 mmol) were added to these solutions sequentially. The resulting mixtures were shaken at room temperature overnight. The solutions were filtered through a bed of Celite and collected into 16 × 100 mm test tubes. Solvents were removed by vacuum centrifugation in a speedvac to afford crude products which were used for the subsequent reaction without further purification.

1-(2,4-Difluorophenyl)-3-(2-phenoxy pyridin-3-yl)ureas (11). To these 3-amino-2-phenoxy pyridines **9** (0.085 mmol) in 2-dram vials was added 2,4-difluorophenyl isocyanate **10** (0.127 mmol) in anhydrous toluene (1 mL). The reaction mixtures were heated with shaking at 80 °C for 1.5 h. Solvents were removed by vacuum centrifugation in a speedvac, and the crude products were purified by reverse phase preparative HPLC.

1-(2,4-Difluorophenyl)-3-(2-phenoxy pyridin-3-yl)urea (11a). Yield: 11.9 mg (35%). ^1H NMR (500 MHz, CD_3OD) δ 6.94 (t, $J = 8.80$ Hz, 1 H), 7.01 (ddd, $J = 11.41, 8.66, 3.02$ Hz, 1 H), 7.09 (dd, $J = 8.25, 4.95$ Hz, 1 H), 7.15 (d, $J = 8.25$ Hz, 2 H), 7.22 (t, $J = 7.42$ Hz, 1 H), 7.42 (t, $J = 7.97$ Hz, 2 H), 7.69 (d, $J = 4.95$ Hz, 1 H), 8.08 (td, $J = 9.07, 6.05$ Hz, 1 H), 8.61 (d, $J = 7.70$ Hz, 1 H). LC-MS (ESI) m/z 342.2 ($M + H^+$); orthogonal HPLC column 1 retention time = 11.05 min, column 2 = 9.47 min.

1-(2-(2-*tert*-Butylphenoxy)pyridin-3-yl)-3-(2,4-difluorophenyl)urea (11b). Yield: 17.5 mg (44%). ^1H NMR (500 MHz, CD_3OD) δ 1.40 (s, 9 H), 6.86 (d, $J = 8.25$ Hz, 1 H), 6.94 (t, $J = 8.80$ Hz, 1 H), 7.01 (ddd, $J = 11.27, 8.52, 3.30$ Hz, 1 H), 7.06 (dd, $J = 7.97, 4.67$ Hz, 1 H), 7.13–7.19 (m, 1 H), 7.20–7.24 (m, 1 H), 7.48 (d, $J = 7.70$ Hz, 1 H), 7.68 (d, $J = 4.95$ Hz, 1 H), 8.07 (td, $J = 9.07, 5.50$ Hz, 1 H), 8.56 (d, $J = 7.70$ Hz, 1 H). LC-MS (ESI) m/z 398.2 ($M +$

H⁺); orthogonal HPLC column 1 retention time = 12.78 min, column 2 = 10.66 min.

1-(2-(3-*tert*-Butylphenoxy)pyridin-3-yl)-3-(2,4-difluorophenyl)urea (11c). Yield: 15.9 mg (40%). ¹H NMR (500 MHz, CD₃OD) δ 1.33 (s, 9 H), 6.91–6.96 (m, 2 H), 7.01 (ddd, J = 11.27, 8.52, 3.30 Hz, 1 H), 7.08 (dd, J = 7.70, 4.95 Hz, 1 H), 7.19 (s, 1 H), 7.26–7.30 (m, 1 H), 7.34 (t, J = 7.97 Hz, 1 H), 7.69 (d, J = 3.30 Hz, 1 H), 8.08 (td, J = 9.21, 5.77 Hz, 1 H), 8.61 (d, J = 8.25 Hz, 1 H). LC-MS (ESI) m/z 398.2 (M + H⁺); orthogonal HPLC column 1 retention time = 13.03 min, column 2 = 10.92 min.

1-(2,4-Difluorophenyl)-3-(2-(2-isopropylphenoxy)pyridin-3-yl)urea (11d). Yield: 16.8 mg (44%). ¹H NMR (500 MHz, CD₃OD) δ 1.20 (d, J = 6.60 Hz, 6 H), 3.12 (t, J = 7.15 Hz, 1 H), 6.94 (t, J = 8.52 Hz, 1 H), 6.99–7.07 (m, 3 H), 7.19–7.29 (m, 2 H), 7.41 (dd, J = 5.77, 3.57 Hz, 1 H), 7.62 (d, J = 4.95 Hz, 1 H), 8.09 (td, J = 9.07, 6.05 Hz, 1 H), 8.57 (d, J = 7.70 Hz, 1 H). LC-MS (ESI) m/z 384.2 (M + H⁺); orthogonal HPLC column 1 retention time = 12.55 min, column 2 = 10.55 min.

1-(2,4-Difluorophenyl)-3-(2-(2-ethylphenoxy)pyridin-3-yl)urea (11e). Yield: 15.7 mg (42%). ¹H NMR (500 MHz, CD₃OD) δ 1.17 (t, J = 7.42 Hz, 3 H), 2.59 (q, J = 7.70 Hz, 2 H), 6.94 (t, J = 8.80 Hz, 1 H), 6.99–7.09 (m, 3 H), 7.16–7.28 (m, 2 H), 7.34 (d, J = 7.70 Hz, 1 H), 7.62 (d, J = 4.95 Hz, 1 H), 8.09 (td, J = 9.07, 6.05 Hz, 1 H), 8.58 (d, J = 7.70 Hz, 1 H). LC-MS (ESI) m/z 370.2 (M + H⁺); orthogonal HPLC column 1 retention time = 12.10 min, column 2 = 10.22 min.

1-(2,4-Difluorophenyl)-3-(2-(2-(trifluoromethyl)phenoxy)pyridin-3-yl)urea (11f). Yield: 13.9 mg (34%). ¹H NMR (400 MHz, CD₃OD) δ 6.99–6.91 (m, 1H), 6.99–6.91 (m, 1H), 7.03 (s, 1H), 7.11 (dd, J = 8.00, 4.90 Hz, 1H), 7.27 (d, J = 8.30 Hz, 1H), 7.44 (s, 1H), 7.74–7.65 (m, 2H), 7.79 (d, J = 7.80 Hz, 1H), 8.09 (d, J = 5.80 Hz, 1H), 8.61 (dd, J = 8.10, 1.80 Hz, 1H). LC-MS (ESI) m/z 410.1 (M + H⁺); orthogonal HPLC column 1 retention time = 12.19 min, column 2 = 10.36 min.

1-(2,4-Difluorophenyl)-3-(2-(4-(trifluoromethyl)phenoxy)pyridin-3-yl)urea (11g). Yield: 13.9 mg (34%). ¹H NMR (500 MHz, CD₃OD) δ 6.94 (t, J = 8.80 Hz, 1 H), 6.98–7.05 (m, 1 H), 7.15 (dd, J = 8.25, 4.95 Hz, 1 H), 7.34 (d, J = 8.80 Hz, 2 H), 7.71–7.77 (m, 3 H), 8.08 (td, J = 9.07, 6.05 Hz, 1 H), 8.65 (d, J = 7.70 Hz, 1 H). LC-MS (ESI) m/z 410.0 (M + H⁺); orthogonal HPLC column 1 retention time = 12.46 min, column 2 = 10.81 min.

1-(2, 4-Difluorophenyl)-3-(2-(4-(methyl)phenoxy)pyridin-3-yl)urea (11h). Yield: 15.3 mg (43%). ¹H NMR (400 MHz, CD₃OD) δ 2.36 (s, 3 H), 6.90–6.97 (m, 1 H), 6.98–7.04 (m, 3 H), 7.06 (dd, J = 8.25, 4.95 Hz, 1 H), 7.23 (d, J = 8.25 Hz, 2 H), 7.66 (d, J = 4.95 Hz, 1 H), 8.08 (td, J = 9.21, 5.77 Hz, 1 H), 8.59 (d, J = 6.05 Hz, 1 H). LC-MS (ESI) m/z 356.2 (M + H⁺); orthogonal HPLC column 1 retention time = 11.67 min, column 2 = 9.91 min.

1-(2-(2-*tert*-Butylphenoxy)pyridin-3-yl)-3-*p*-tolylurea (12). Yield: 8.6 mg (23%). ¹H NMR (500 MHz, CD₃OD) δ 1.39 (s, 9 H), 2.29 (s, 3 H), 6.86 (d, J = 8.25 Hz, 1 H), 7.06 (dd, J = 8.25, 4.95 Hz, 1 H), 7.11 (d, J = 8.80 Hz, 2 H), 7.14–7.19 (m, 1 H), 7.20–7.24 (m, 1 H), 7.32 (d, J = 8.25 Hz, 2 H), 7.48 (d, J = 7.70 Hz, 1 H), 7.66 (d, J = 4.95 Hz, 1 H), 8.56 (d, J = 6.60 Hz, 1 H). LC-MS (ESI) m/z 376.2 (M + H⁺); orthogonal HPLC column 1 retention time = 12.82 min, column 2 = 10.75 min.

Synthesis of 1-(2-(2-*tert*-Butylphenylthio)pyridin-3-yl)-3-*p*-tolylurea (13). To a solution of 2-chloro-3-nitropyridine 3 (158 mg, 1.0 mmol) and 2-*tert*-butylbenzenethiol (166 mg, 1.0 mmol) in DMF (3 mL) was added Cs₂CO₃ (383 mg, 1.2 mmol). The resulting mixture was stirred at 80 °C overnight. The insoluble material was removed by filtration, and the DMF solution was diluted with H₂O (5 mL) and extracted with EtOAc (2 × 6 mL). The EtOAc solution was washed with 5% aq LiCl solution (3 × 3 mL). Drying (MgSO₄) and removal of solvent in vacuo afforded a yellow solid which was triturated with MeOH to yield 2-((2-*tert*-butylphenyl)thio)-3-nitropyridine as a yellow solid (115 mg, 40%). HPLC purity: 100%. This material was used for the next step without further purification.

To a solution of 2-((2-*tert*-butylphenyl)thio)-3-nitropyridine (50 mg, 0.173 mmol) in 1:1 MeOH/EtOAc (3 mL) was added 10%

palladium on activated charcoal (5 mg, 0.0047 mmol). The resulting mixture was stirred at 3.5 atm hydrogen pressure for 1 h. The catalyst was removed by filtration through a bed of Celite, and the solvent was removed by vacuum centrifugation in a speedvac to afford 2-((2-*tert*-butylphenyl)thio)pyridin-3-amine as a yellow solid (33 mg, 74%). (M + H⁺) = 259.1.

To a solution of 2-((2-*tert*-butylphenyl)thio)pyridin-3-amine (33 mg, 0.12 mmol) in anhydrous THF (2 mL) was added *p*-tolyl isocyanate (20 μ L, 0.15 mmol). The resulting mixture was stirred at 60 °C for 1.5 h. The solvent was removed by vacuum centrifugation in a speedvac, and the crude mixture was purified by reverse phase preparative HPLC. After removal of solvent in vacuo, the TFA salt of compound 13 was obtained as a yellow solid (12.5 mg, 27%). ¹H NMR (500 MHz, CDCl₃) δ 1.40 (s, 9 H), 2.28 (s, 3 H), 6.97 (d, J = 7.70 Hz, 1 H), 7.05 (d, J = 7.70 Hz, 2 H), 7.10 (t, J = 7.42 Hz, 1 H), 7.20 (d, J = 7.70 Hz, 2 H), 7.25–7.37 (m, 2 H), 7.49 (d, J = 7.70 Hz, 1 H), 8.15 (d, J = 3.85 Hz, 1 H), 8.74 (d, J = 8.25 Hz, 1 H). LC-MS (ESI) m/z 392.4 (M + H⁺); orthogonal HPLC column 1 retention time = 13.12 min, column 2 = 10.95 min.

1-(2-(2-*tert*-Butylphenylamino)pyridin-3-yl)-3-*p*-tolylurea (14). To a solution of 2-chloro-3-nitropyridine 3 (1.58 g, 10 mmol) and 2-*tert*-butylaniline (1.79 g, 12 mmol) in dioxane (50 mL) was added NEt₃ (1.21 g, 12 mmol). The resulting solution was reflux for 16 h, and solvent was evaporated in vacuo to afford a yellow solid which was recrystallized from MeOH to give *N*-(2-*tert*-butylphenyl)-3-nitropyridin-2-amine (1.98 g, 73%) as a yellow solid. (M + H⁺) = 272.1.

The *N*-(2-(*tert*-butylphenyl)-3-nitropyridin-2-amine (272 mg, 1 mmol) was then dissolved in a 4:1 mixed solution containing absolute EtOH (4 mL) and EtOAc (1 mL). Zn dust (1.3 g, 20 mmol) and NH₄Cl (300 mg, 5.4 mmol) were added to this solution sequentially. The resulting mixture was stirred at room temperature overnight. The solution was filtered through a bed of Celite, and the solvent was evaporated in vacuo to afford the N²-(2-*tert*-butylphenyl)pyridine-2,3-diamine (242 mg, 100%) as solid. (M + H⁺) = 242.1. This material was used for the next step without further purification.

To a solution of N²-(2-*tert*-butylphenyl)pyridine-2,3-diamine (24.2 mg, 0.1 mmol) in anhydrous THF (1 mL) in a 1-dram vial was added *p*-tolyl isocyanate (20 μ L, 0.15 mmol). The resulting mixture was stirred at 60 °C for 1.5 h. The solvent was removed by vacuum centrifugation in a speedvac, and the crude mixture was purified by reverse phase preparative HPLC. After removal of solvent in vacuo, the TFA salt of compound 14 was obtained as a white solid (15.3 mg, 41%). ¹H NMR (500 MHz, CDCl₃) δ 1.26 (s, 9 H), 2.27 (s, 3 H), 6.70–6.76 (m, 1 H), 6.95 (d, J = 7.70 Hz, 1 H), 7.04 (d, J = 8.25 Hz, 2 H), 7.14–7.22 (m, 2 H), 7.24–7.30 (m, 1 H), 7.35 (d, J = 8.25 Hz, 2 H), 7.48 (d, J = 7.70 Hz, 1 H), 8.47 (d, J = 7.70 Hz, 1 H), 9.08 (br s, 1 H), 9.94 (d, J = 6.60 Hz, 1 H), 10.05 (br s, 1 H). LC-MS (ESI) m/z 375.2 (M + H⁺); orthogonal HPLC column 1 retention time = 7.13 min, column 2 = 7.95 min.

1-(2-(2-(2-*tert*-Butylphenyl)(methyl)amino)pyridin-3-yl)-3-*p*-tolylurea (15). To a solution of *N*-(2-*tert*-butylphenyl)-3-nitropyridin-2-amine (816 mg, 3 mmol) in anhydrous THF (6 mL) was added 60% NaH (360 mg, 9 mmol) followed by iodomethane (2.56 g, 18 mmol). After the mixture was stirred at 60 °C for 24 h, an additional 3 equiv of iodomethane (1.28 g, 9 mmol) was added. Stirring was continued at 60 °C for an additional 48 h. The reaction mixture was allowed to cool to room temperature, and solvent was evaporated to afford a crude mixture which was purified by reverse phase preparative HPLC. Removal of solvent afforded a yellow oil which was dissolved in EtOAc (20 mL) and washed with NaHCO₃. Drying (MgSO₄) and removal of solvent afforded the *N*-(2-*tert*-butylphenyl)-*N*-methyl-3-nitropyridin-2-amine (427 mg, 50%) as a light yellow oil. (M + H⁺) = 286.1.

To a solution of *N*-(2-*tert*-butylphenyl)-*N*-methyl-3-nitropyridin-2-amine (427 mg, 1.5 mmol) in EtOH (10 mL) was added 10% palladium on activated charcoal (50 mg, 0.047 mmol). The resulting solution was stirred under 1 atm hydrogen pressure for 48 h. The solution was filtered through a bed of Celite, and the solvent was evaporated in vacuo to afford the N²-(2-*tert*-butylphenyl)-N²-

methylpyridine-2,3-diamine (267 mg, 70%) as a dark oil. ($M + H^+$) = 256.1. This material was used for the next step without further purification.

To a solution of N^2 -(2-*tert*-butylphenyl)- N^2 -methylpyridine-2,3-diamine (25.5 mg, 0.1 mmol) in anhydrous THF (1 mL) in a 1-dram vial was added *p*-tolyl isocyanate (20 μ L, 0.15 mmol). The resulting mixture was stirred at 60 °C for 1.5 h. The solvent was removed by vacuum centrifugation in a speedvac, and the crude mixture was purified by reverse phase preparative HPLC. After removal of solvent in vacuo TFA salt of compound 15 was obtained as a white solid (8.9 mg, 23%). 1H NMR (500 MHz, DMSO- d_6) δ 1.28 (s, 9 H), 2.21 (s, 3 H), 3.19 (s, 3 H), 6.80 (dd, J = 7.70, 4.95 Hz, 1 H), 6.96–7.07 (m, 3 H), 7.12–7.23 (m, 4 H), 7.40–7.52 (m, 2 H), 7.98 (d, J = 4.40 Hz, 1 H), 8.59 (br s, 1 H). LC-MS (ESI) m/z 389.3 ($M + H^+$); orthogonal HPLC column 1 retention time = 7.43 min, column 2 = 8.15 min.

1-(2-(2-*tert*-Butylphenoxy)pyridin-3-yl)-3-(4-(trifluoromethoxy)phenyl)urea (16). Yield: 15.1 mg (34%). 1H NMR (500 MHz, CD_3OD) δ 1.41 (s, 9 H), 7.05–7.12 (m, 1 H), 7.21 (d, J = 8.80 Hz, 2 H), 7.30–7.37 (m, 2 H), 7.43 (dd, J = 8.25, 5.50 Hz, 1 H), 7.54–7.66 (m, 3 H), 7.81 (d, J = 5.50 Hz, 1 H), 9.06 (d, J = 8.25 Hz, 1 H). ^{13}C NMR (125 MHz, CD_3OD) δ 29.81, 34.26, 118.68, 119.37, 119.80, 121.42, 121.90, 123.03, 124.64, 125.14, 126.96, 127.21, 127.81, 138.21, 139.10, 141.63, 144.14, 144.16, 152.82, 153.36, 153.42. LC-MS (ESI) m/z 446.1 ($M + H^+$); orthogonal HPLC column 1 retention time = 12.37 min, column 2 = 12.78 min.

1-(2-(2-*tert*-Butylphenoxy)pyridin-3-yl)-3-(4-*tert*-butylphenyl)urea (17). Yield: 19.2 mg (46%). 1H NMR (500 MHz, CD_3OD) δ 1.30 (s, 9 H), 1.40 (s, 9 H), 6.91 (d, J = 7.70 Hz, 1 H), 7.14 (dd, J = 7.97, 5.22 Hz, 1 H), 7.18–7.22 (m, 1 H), 7.25 (t, J = 7.70 Hz, 1 H), 7.32–7.39 (m, 4 H), 7.51 (d, J = 7.70 Hz, 1 H), 7.69 (d, J = 5.50 Hz, 1 H), 8.68 (d, J = 7.70 Hz, 1 H). LC-MS (ESI) m/z 418.2 ($M + H^+$); orthogonal HPLC column 1 retention time = 12.68 min, column 2 = 11.02 min.

1-(4-*tert*-Butylphenyl)-3-(2-(2-isopropylphenoxy)pyridin-3-yl)urea (18). Yield: 25.4 mg (63%). 1H NMR (500 MHz, CD_3OD) δ 1.20 (d, J = 6.05 Hz, 6 H), 1.31 (s, 9 H), 3.06–3.17 (m, 1 H), 6.97–7.01 (m, 1 H), 7.03 (dd, J = 7.70, 4.95 Hz, 1 H), 7.24 (dd, J = 5.50, 3.30 Hz, 2 H), 7.32–7.39 (m, 4 H), 7.40–7.44 (m, 1 H), 7.60 (d, J = 4.95 Hz, 1 H), 8.57 (d, J = 7.70 Hz, 1 H). LC-MS (ESI) m/z 404.2 ($M + H^+$); orthogonal HPLC column 1 retention time = 13.52 min, column 2 = 12.00 min.

1-(2-(2-Isopropylphenoxy)pyridin-3-yl)-3-(4-(trifluoromethoxy)phenyl)urea (19). Yield: 24.1 mg (57%). 1H NMR (500 MHz, $CDCl_3$) δ 1.25–1.16 (m, 6H), 3.07 (dt, J = 13.60, 6.70 Hz, 1H), 7.05 (d, J = 8.20 Hz, 1H), 7.15 (s, 2H), 7.36–7.22 (m, 3H), 7.42 (d, J = 7.70 Hz, 1H), 7.55 (d, J = 3.30 Hz, 2H), 7.74 (d, J = 4.90 Hz, 1H), 9.11 (dd, J = 14.80, 8.20 Hz, 1H). LC-MS (ESI) m/z 424.3 ($M + H^+$); orthogonal HPLC column 1 retention time = 12.32 min, column 2 = 12.73 min.

P2Y₁ Binding Assay. The P2Y₁ binding assay was used to identify inhibitors of [β -³³P]-2MeS-ADP binding to cloned human P2Y₁ receptors. The cDNA clone for human P2Y₁ was obtained from Incyte Pharmaceuticals and its sequence confirmed by established techniques (for a compendium of techniques used, see Ausubel, F. et al. *Current Protocols in Molecular Biology*; John Wiley and Sons: New York, 1995). The essential coding sequences were subcloned into pCDNA 3.1 (Invitrogen) to produce a P2Y₁ expression construct. This construct was then transfected into the human embryonic kidney cell line HEK-293, and stable transfectants were selected in GENETICIN (G418 sulfate; Life Technologies). Several lines were screened for binding activity, and one (HEK293 #49) was selected for further characterization. Membranes were prepared by growing HEK293 #49 in 150 mm dishes in DMEM/10% FBS in the presence of 1 mg/mL G418 until cells were 80–90% confluent. Plates were then washed with cold (4 °C) D-PBS twice and cells harvested by scraping into 10 mL of D-PBS. Cells were pelleted by centrifugation (1000g, 10 min, 4 °C), and the resulting pellet was resuspended in lysis buffer (10 mM Tris (7.4), 5 mM MgCl₂ containing Complete protease inhibitor cocktail (Roche cat. no. 1873580). The suspension was then homogenized in a Dounce homogenizer (10–15 strokes; B pestle,

on ice) and the homogenate spun at 1000g, 4 °C, 5 min to pellet large debris. The supernatant was centrifuged at 150 000g, 4 °C, for 1 h and the resulting membrane pellet resuspended in 0.5–1 mL of buffer B (15 mM HEPES (7.4), 145 mM NaCl, 0.1 mM MgCl₂, 5 mM EDTA, 5 mM KCl), and stored at –70 °C until used. A typical procedure which was adequate for solubilizing all urea compounds consisted of adding a 10 μ L aliquot of DMSO containing the test compound diluted to the final assay concentrations of 0.01 nM to 1 mM in the bottom of a 96-well WGA Flashplate (NEN) and adding 190 μ L of assay buffer containing sufficient [β -³³P]-2MeS-ADP and membrane preparation to produce final concentrations of 0.5 nM and 0.025 μ g/ μ L, respectively. Binding reactions were allowed to proceed to completion at room temperature for 1 h, and then the aqueous solution was aspirated. Plates were sealed, and the residual [β -³³P] bound to the plate was determined by scintillation counting. Dose–response curves (IC₅₀) were fit by nonlinear regression (XLFit, ID Business Solutions Ltd.) and binding constants (K_i) calculated using the Cheng–Prusoff relationship ($K_i = IC_{50}/(1 + L/K_d)$) in which a K_d for 2MeS-ADP to the P2Y₁ receptor was determined to be 14 nM).

P2Y₁₂ Binding Assay. The P2Y₁₂ cell binding assay is designed for testing compound selectivity. The cDNA of P2Y₁₂ was obtained from Incyte Pharmaceuticals and its sequence confirmed by established technique. The essential coding sequences were subcloned into pCDNA 3.1 (Invitrogen) to produce a P2Y₁₂ expression construct. This construct was then transfected into the human embryonic kidney cell line HEK-293, and transfected cells were selected in hygromycin B (Invitrogen cat. no. 10687-010).

HEK293-P2Y₁₂ cells (50K/well) in a 50 μ g/mL poly-D-lysine-precoated 96-well assay plate (Costar cat. no. 3917) with selective medium (0.5 mg/mL hygromycin, 10% FBS, DMEM) were plated overnight. The cell culture medium was aspirated, and the cells were washed with 100 μ L of serum-free DMEM once. Then 98 μ L of serum-free DMEM, 2 μ L of compound solution, and 100 μ L of 1 nM [β -³³P]-2MeS-ADP were added to each well. The assay plate was incubated at 5% CO₂, 37 °C, for 1 h. At the end of the incubation, the aqueous medium was aspirated and the cells were washed with 200 μ L of DPBS twice. The assay plate was dried by inverting it on a paper towel, 100 μ L of scintillation fluid (Ultima Gold, Perkin-Elmer cat. no. 603329) was added to each well, and the assay plate was shaken for 15 min. [β -³³P] bound to the cells was determined by scintillation counting in TopCount. Dose–response curves (IC₅₀) were fit by nonlinear regression (XLFit, ID Business Solutions Ltd.), and binding constants (K_i) were calculated using the Cheng–Prusoff relationship ($K_i = IC_{50}/(1 + L/K_d)$) in which a K_d for 2MeS-ADP to the P2Y₁₂ receptor was determined to be 1.4 nM.

AUTHOR INFORMATION

Corresponding Author

*Phone: 609-818-5413. Fax: 609-818-3450. E-mail: Hannguang.chao@bms.com.

Notes

The authors declare no competing financial interest.

ABBREVIATIONS USED

ADP, adenosine diphosphate; AUC, area under curve; CL, clearance; iv, intravenous; HEK, human embryonic kidney; HPLC, high-pressure liquid chromatography; metab stab., metabolic stability; po, per os (by mouth); PRP, platelet-rich plasma; P2Y, G-protein-coupled purinergic receptors; SAR, structure–activity relationship; TFA, trifluoroacetic acid; V_{ss} , volume of distribution; WGA, wheat germ agglutinin

REFERENCES

(1) Janssens, R.; Communi, D.; Piroton, S.; Samson, M.; Parmentier, M.; Boeynaems, J. M. Cloning and Tissue Distribution of the Human P2Y₁ Receptor. *Biochem. Biophys. Res. Commun.* **1996**, 221, 588–593.

- (2) (a) Boeynaems, J. M.; Bernard, R.; Rodolphe, J.; Nathalie, S.-H.; Didier, C. Overview of P2Y Receptors as Therapeutic Targets. *Drug Dev. Res.* **2001**, *52*, 187–189. (b) Abbracchio, M. P.; Burnstock, G.; Boeynaems, J. M.; Barnard, E. A.; Boyer, J. L.; Kennedy, C.; Knight, G. E.; Fumagalli, M.; Gachet, C.; Jacobson, K. A.; Weisman, G. A. International Union of Pharmacology LVIII: Update on the P2Y G Protein-Coupled Nucleotide Receptors: from Molecular Mechanisms and Pathophysiology to Therapy. *Pharmacol. Rev.* **2006**, *58*, 281–341.
- (3) (a) Burnstock, G.; Williams, M. P2 Purinergic Receptors: Modulation of Cell Function and Therapeutic Potential. *J. Pharm. Exp. Ther.* **2000**, *295*, 862–869. (b) Jacobson, K. A.; Boeynaems, J.-M. P2Y Nucleotide Receptors: Promise of Therapeutic Applications. *Drug Discovery Today* **2010**, *15*, 570–578. (c) Govindan, S.; Taylor, C. W. P2Y Receptor Subtypes Evoke Different Ca^{2+} Signals in Cultured Aortic Smooth Muscle Cells. *Purinergic Signalling* **2012**, *8*, 763–777. (d) Jacobson, K. A.; Jayasekara, M. P.; Costanzi, S. Molecular Structure of P2Y Receptors: Mutagenesis, Modeling, and Chemical Probes. *WIREs Membr. Transp. Signaling* **2012**, *1*, 815–827.
- (4) (a) Abbracchio, M. P.; Burnstock, G. Purinoceptors: Are There Families of P2X and P2Y Purinoceptors? *Pharmacol. Ther.* **1994**, *64*, 445–475. (b) Wihlborg, A.-K.; Balogh, J.; Wang, L.; Borna, C.; Dou, Y.; Joshi, B. V.; Lazarowski, E.; Jacobson, K. A.; Arner, A.; Erlinge, D. Positive Inotropic Effects by Uridine Triphosphate (UTP) and Uridine Diphosphate (UDP) via P2Y₂ and P2Y₆ Receptors on Cardiomyocytes and Release of UTP in Man During Myocardial Infarction. *Circ. Res.* **2006**, *98*, 970–976. (c) Raju, N. C.; Eikelboom, J. W.; Hirsh, J. Platelet ADP-Receptor Antagonists for Cardiovascular Disease: Past, Present and Future. *Nat. Clin. Pract. Cardiovasc. Med.* **2008**, *5*, 766–780.
- (5) Hollopeter, G.; Jantzen, H. M.; Vincent, D.; Li, G.; England, L.; Ramakrishnan, V.; Yang, R.-B.; Nurden, P.; Nurden, A.; Julius, D.; Conley, P. B. Identification of the Platelet ADP Receptor Targeted by Antithrombotic Drugs. *Nature* **2001**, *409*, 202–207.
- (6) (a) Pereillo, J. M.; Maftouh, M.; Andrieu, A.; Uzabiaga, M. F.; Fedeli, O.; Savi, P.; Pascal, M.; Herbert, J. M.; Maffrand, J. P.; Picard, C. Structure and Stereochemistry of the Active Metabolite of Clopidogrel. *Drug Metab. Dispos.* **2002**, *30*, 1288–1295. (b) Husted, S.; Emanuelsson, H.; Heptinstall, S.; Sandset, P. M.; Wickens, M.; Peters, G. Pharmacodynamics, Pharmacokinetics, and Safety of the Oral Reversible P2Y₁₂ Antagonist AZD6140 with Aspirin in Patients with Atherosclerosis: a Double-Blind Comparison to Clopidogrel with Aspirin. *Eur. Heart J.* **2006**, *27*, 1038–1047. (c) Jernberg, T.; Payne, C. D.; Winters, K. J.; Darstein, C.; Brandt, J. T.; Jakubowski, J. A.; Naganuma, H.; Siegbahn, A.; Wallentin, L. Prasugrel Achieves Greater Inhibition of Platelet Aggregation and a Lower Rate of Non-Responders Compared with Clopidogrel in Aspirin-Treated Patients with Stable Coronary Artery Disease. *Eur. Heart J.* **2006**, *27*, 1166–117. (d) Jakubowski, J. A.; Winters, K. J.; Naganuma, H.; Wallentin, L. Prasugrel: a Novel Thienopyridine Antiplatelet Agent. A Review of Preclinical and Clinical Studies and the Mechanistic Basis for its Distinct Antiplatelet Profile. *Cardiovasc. Drug Rev.* **2007**, *25*, 357–374.
- (7) For cangrelor, see: (a) Ingall, A. H.; Dixon, J.; Bailey, A.; Coombs, M. E.; Cox, D.; McNally, J. I.; Hunt, S. F.; Kindon, N. D.; Teobald, B. J.; Willis, P. A.; Humphries, R. G.; Leff, P.; Clegg, J. A.; Smith, J. A.; Tomlinson, W. Antagonists of the Platelet P2T Receptor: a Novel Approach to Antithrombotic Therapy. *J. Med. Chem.* **1999**, *42*, 213–220. (b) Humphries, R. G.; Tomlinson, W.; Ingall, A. H.; Cage, P. A.; Leff, P. FPL 66096: a Novel, Highly Potent and Selective Antagonist at Human Platelet P2T-Purinoreceptors. *Br. J. Pharmacol.* **1994**, *113*, 1057–1063. For ticagrelor, see: (c) Springthorpe, B.; Bailey, A.; Barton, P.; Birkinshaw, T. N.; Bonnert, R. V.; Brown, R. C.; Chapman, D.; Dixon, J.; Guile, S. D.; Humphries, R. G.; Hunt, S. F.; Ince, F.; Ingall, A. H.; Kirk, I. P.; Leeson, P. D.; Leff, P.; Lewis, R. J.; Martin, B. P.; McGinnity, D. F.; Mortimore, M. P.; Paine, S. W.; Pairaudeau, G.; Patel, A.; Rigby, A. J.; Riley, R. J.; Teobald, B. J.; Tomlinson, W.; Webborn, P. J. H.; Willis, P. A. From ATP to AZD6140: The Discovery of an Orally Active Reversible P2Y₁₂ Receptor Antagonist for the Prevention of Thrombosis. *Bioorg. Med. Chem. Lett.* **2007**, *17*, 6013–6018. (d) Cattaneo, M. New P2Y₁₂ Inhibitors. *Circulation* **2010**, *121*, 171–179.
- (8) Léon, C.; Freund, M.; Ravanat, C.; Baurand, A.; Cazenave, J. P.; Gachet, C. Key Role of the P2Y₁ Receptor in Tissue Factor–Induced Thrombin-Dependent Acute Thromboembolism: Studies in P2Y₁-Knockout Mice and Mice Treated With a P2Y₁ Antagonist. *Circulation* **2001**, *103*, 718–723.
- (9) (a) Boyer, J. L.; Mohanram, A.; Camaioni, E.; Jacobson, K. A.; Harden, T. K. Competitive and Selective Antagonism of P2Y₁ Receptors by N6-Methyl 2'-Deoxyadenosine 3',5'-Bisphosphate. *Br. J. Pharmacol.* **1998**, *124*, 1–3. (b) Tantry, U. S.; Bliden, K. P.; Gurbel, P. A. AZD6140. *Expert Opin. Invest. Drugs* **2007**, *16*, 225–229.
- (10) For MRS2179, see: (a) Camaioni, E.; Boyer, J. L.; Mohanram, A.; Harden, T. K.; Jacobson, K. A. Deoxyadenosine Bisphosphate Derivatives as Potent Antagonists at P2Y₁ Receptors. *J. Med. Chem.* **1998**, *41*, 183–190. For MRS2500, see: (b) Kim, H. S.; Ohno, M.; Xu, B.; Kim, H. O.; Choi, Y.; Ji, X. D.; Maddileti, S.; Marquez, V. E.; Harden, T. K.; Jacobson, K. A. Modeling the Adenosine Receptors: Comparison of the Binding Domains of A2A Agonists and Antagonists. *J. Med. Chem.* **2003**, *46*, 4847–4859. For examples of other P2Y₁ antagonists, see: (c) Nandanan, E.; Jang, S.-Y.; Moro, S.; Kim, H. O.; Siddiqui, M. A.; Russ, P.; Marquez, V. E.; Busson, R.; Herdewijn, P.; Harden, T. K.; Boyer, J. L.; Jacobson, K. A. Synthesis, Biological Activity, and Molecular Modeling of Ribose-Modified Deoxyadenosine Bisphosphate Analogues as P2Y₁ Receptor Ligands. *J. Med. Chem.* **2000**, *43*, 829–842. (d) Kim, H. S.; Barak, D.; Harden, T. K.; Boyer, J. L.; Jacobson, K. A. Acyclic and Cyclopropyl Analogues of Adenosine Bisphosphate Antagonists of the P2Y₁ Receptor: Structure–Activity Relationships and Receptor Docking. *J. Med. Chem.* **2001**, *44*, 3092–3108. (e) Nahum, V.; Zundorf, G.; Levesque, S. A.; Beaudoin, A. R.; Reiser, G.; Fischer, B. Adenosine 5'-O-(1-Boranotriphosphate) Derivatives as Novel P2Y₁ Receptor Agonists. *J. Med. Chem.* **2002**, *45*, 5384–5396. (f) Nahum, V.; Tulapurkar, M.; Levesque, S. A.; Seigny, J.; Reiser, G.; Fischer, B. Diadenosine and Diuridine Poly(borano)phosphate Analogues: Synthesis, Chemical and Enzymatic Stability, and Activity at P2Y₁ and P2Y₂ Receptors. *J. Med. Chem.* **2006**, *49*, 1980–1990.
- (11) For examples on nonnucleotide P2Y₁ receptor antagonists, see: (a) Chao, H.; Turdi, H.; Herpin, T. F.; Roberge, J. Y.; Liu, Y.; Lawrence, R. M.; Rehffuss, R. P.; Clark, C. G.; Qiao, J. X.; Gungor, T.; Lam, P. Y.; Wang, T.; Ruel, R.; L'Heureux, A.; Thibeault, C.; Bouthillier, G.; Schnur, D. Preparation of Phenyl or Pyridinyl Ureas as Antagonists of P2Y₁ Receptors for the Treatment of Thromboembolic Disorders. WO2005/113351 A1, 2005. (b) Pfefferkorn, J. A.; Choi, C.; Winters, T.; Kennedy, R.; Chi, L.; Perrin, L. A.; Lu, G.; Ping, Y.-W.; McClanahan, T.; Schroeder, R.; Leininger, M. T.; Geyer, A.; Schefzick, S.; Atherton, J. P2Y₁ Receptor Antagonists as Novel Antithrombotic Agents. *Bioorg. Med. Chem. Lett.* **2008**, *18*, 3338–3343. (c) Morales-Ramos, A. I.; Mecom, J. S.; Kiesow, T. J.; Graybill, T. L.; Brown, G. D.; Aiyar, N. V.; Davenport, E. A.; Kallal, L. A.; Knapp-Reed, B. A.; Li, P.; Londregan, A. T.; Morrow, D. M.; Senadhi, S.; Thalji, R. K.; Zhao, S.; Burns-Kurtis, C. L.; Marino, J. P., Jr. Tetrahydro-4-quinolinamines Identified as Novel P2Y(1) Receptor Antagonists. *Bioorg. Med. Chem. Lett.* **2008**, *18*, 6222–6226. (d) Thalji, R. K.; Aiyar, N.; Davenport, E. A.; Erhardt, J. A.; Kallal, L. A.; Morrow, D. M.; Senadhi, S.; Burns-Kurtis, C. L.; Marino, J. P., Jr. Benzofuran-Substituted Urea Derivatives as Novel P2Y₁ Receptor Antagonists. *Bioorg. Med. Chem. Lett.* **2010**, *20*, 4104–4107. (e) Costanzi, S.; Kumar, T. S.; Balasubramanian, R.; Harden, T. K.; Jacobson, K. A. Virtual Screening Leads to the Discovery of Novel Non-nucleotide P2Y₁ Receptor Antagonists. *Bioorg. Med. Chem. Lett.* **2010**, *20*, 5254–5261.
- (12) Schumacher, W. A.; Bostwick, J. S.; Ogletree, M. L.; Stewart, A.; Steinbacher, T. E.; Hua, J.; Price, L.; Wong, P. C.; Rhesfuss, R. Biomarker Optimization to Track the Antithrombotic and Hemostatic Effects of Clopidogrel in Rats. *J. Pharmacol. Exp. Ther.* **2007**, *322*, 369–377.
- (13) Sigurdsson, S.; Seeger, B.; Kutzke, U.; Eckstein, F. A Mild and Simple Method for the Preparation of Isocyanates from Aliphatic Amines Using Trichloromethyl Chloroformate. Synthesis of an

Isocyanate Containing an Activated Disulfide. *J. Org. Chem.* **1996**, *61*, 3383–3384.

(14) Platelet aggregation assays were performed in PRP as described in *Platelet Protocols: Research and Clinical Laboratory Procedures*; White, M. M., Jennings, L. K., Eds.; Academic Press: New York, 1999, using 30 μ M agatrobaban (GSK) as the anticoagulant and 2.5 μ M ADP as the agonist. Aggregation data were analyzed as area under the curve (AUC) for 5 min.

(15) Other P2Y₁₂ antagonists have also shown a superior antithrombotic/bleeding profile relative to clopidogrel in rat thrombosis models similar to those described here. See Van Giezen, J. J. J.; Berntsson, P.; Zachrisson, H.; Björkman, J.-A. Comparison of Ticagrelor and Thienopyridine P2Y₁₂ Binding Characteristics and Antithrombotic and Bleeding Effects in Rat and Dog Models of Thrombosis/Hemostasis. *Thromb. Res.* **2009**, *124*, 565–571.